Uptake of Arsenic and Lead ions by the adsorbent material prepared from physiochemical modification of spinach leaves

Brijesh Kumar Das* and Vinay Kumar Jha*

*Central Department of Chemistry, Tribhuvan University, Kirtipur, Kathmandu, Nepal.

Abstract: Physiochemically modified adsorbent material from spinach was prepared by refluxing for 12, 24 and 36 hours in *ortho* phosphoric acid solution with in the temperature range between 60 - 100 °C. The highest specific surface area of 436 m^2/g was obtained with refluxing for 24 hours sample (SA-24) and was selected for the adsorption of As(III) and Pb(II) ions from the aqueous solution with varying several parameters such as pH, kinetics, and concentration of adsorbent.

The adsorbent before and after adsorption of As(III) and Pb(II) was characterized by FTIR and XRD. Studies showed that the maximum efficiency at pH 5 for As(III) and Pb(II). Kinetics and isotherm model studies demonstrated that the experimental data fitted with pseudo-second order and Langmuir isotherm model with the rate constants 2.495 and 0.039 g/(mg·min) and the maximum adsorption capacities 116.28 and 128.21 mg/g for As(III) and Pb(II), respectively. The negative free energy (ΔG values -23 and -25 kJ/mol for As(III) and Pb(II), respectively) in adsorption process revealed the spontaneous nature and feasibility of the adsorption process onto spinach adsorbent. The values of ΔG further confirmed that the adsorption process was favored by physiochemical adsorption for As(III) and Pb(II), respectively.

Keywords: Freundlich isotherm; Langmuir isotherm; Optical micrograph; Reflux; Spinach adsorbent.

Introduction

Drinking water is very much precious for living beings. Everyone on this planet has a right to have pure and safe drinking water. This not only helps a person in satisfying his/her thirst but also offer healthy results to the body. However, the natural sources of the water are shrinking as per the population is rising and resulting the supply of impure water. Just boiling water does not guarantee its freshness and germ free[1].

In major cities of Nepal, health related problems such as cholera, typhoid and jaundice are increasing rapidly and small children are also getting affected because of the same. This is why, it is recommended to use water purifiers beside the marketing strategy, it is to understand by the house holds that it is the need for safe and pure drinking water. Not only this is important for you but also important for children as they came in contact with the dust and air pollution directly every day[2].

Water is the most important resources for the existence of the life in earth, Due to the urbanization, industrialization and rapid population growth, water is being polluted day by day. More than 2.6 billion people (40%) of the world's population lack basic sanitation facilities and one billion people still have unsafe drinking water sources[3]. Even though out of total population of Nepal an estimated 84% have access to drinking water, which is not safe. In rural areas of Nepal, millions of people do not have access to safe drinking water or basic sanitation sources only 27% of the population as a whole has access to sanitary facilities[2].

Most rivers in Nepal's urban area have been polluted and their water are now unfitted for human use, whereas drinking water in Kathmandu is contaminated with coliform bacteria, iron, ammonia and other contaminates[4].

Author for Correspondence: Vinay Kumar Jha, Central Department of Chemistry, Tribhuvan University, Kirtipur, Kathmandu, Nepal.
Email: vinayj2@yahoo.com; https://orcid.org/0000-0001-6375-8482

Received: 24 Mar, 2024; Received in revised form: 20 Apr, 2024; Accepted: 01 May 2024.
Doi: https://Doi.org/10.3126/sw.v17i17.66436

An earthquake of magnitude 9.0 struck eastern Japan on March 11, 2011. The Tokyo Electric Power Company's Fukushima Daiichi Nuclear Power Station suffered serious damage from resulting tsunami and large amount of radio nuclides were released into environment these radio nuclei fell to the ground with dust, rain or snow, contaminating agriculture land and crops. Since the power station was located and in spinach producing Ibaraki prefecture, the study showed the maximum level of heavy metal and radioactive nuclides were being absorbed by spinach plants[5].

Environmental pollution with heavy metals has become a global phenomenon as a consequence of industrial and metallurgical process which introduce majority of toxic chemicals into the environment[6].

The heavy metals of widespread concern to human health are lead, copper, mercury, cadmium, arsenic, chromium, as well as zinc[7].

Lead is a toxic element that occurs naturally in rocks, soil, plants, water, and the atmosphere. Lead has been used in many products such as in anti-knock compound, gasoline, pesticides, paints, and storage batteries. It can be harmful to humans when inhaled, ingested directly through the consumption of contaminated water, or ingested indirectly by consuming crops grown on contaminated soils or irrigated with contaminated water. Diseases such as neurobehavioral impairment, hypertension, and cardiovascular disease in humans are attributed to excessive Pb exposure, especially in growing children[8].

Arsenic is a ubiquitous element that is found naturally in the environment. Inorganic arsenite (As^{3+}) and arsenate (As^{5+}) are the dominant toxic As species found in food and drinking water. High exposure to As has been shown to cause skin, lung and bladder cancer in humans. Humans can be exposed to As directly through the consumption of water and indirectly by consuming crops grown on As contaminated soils or irrigated with contaminated water. It has been estimated that 35 to 77 million people in Bangladesh are at risk of As poisoning from drinking As contaminated well water. The major pathway for human As contamination is the consumption of drinking water. The recommended guideline set by Environmental Protection Agency (EPA) for As in drinking water is 10 μgL^{-1}, but it currently has no recommended guidelines for As in food crops[8].

Various conventional methods have been developed like chemical precipitation, chemical oxidation and reduction, ion exchange, filtration, electrochemical treatment and evaporative recovery for the removal of heavy metals from contaminated wastewaters. However, these methods have certain performance limitations like often being inefficient, expensive, or generating large amount of sludge and other waste products that require further disposal[9].

Batch and column operation were performed utilizing thioglycoalated sugarcane to remove As(III) and As(V) from the aqueous solution and it was found that the maximum removal of As(III) and As(V) species from arsenic spiked distilled water were 85.01 and 83.82 μg/g, respectively. The optimum adsorption was observed at pH 6[10].

The arsenic ion adsorption study on the adsorbent obtained from spinach leaves by activating with H_2SO_4 was done in a study. The adsorption process was fitted to Langmuir adsorption isotherm model with equilibrium adsorption capacity 58.480 mg/g and controlled by pseudo-second–order kinetics where the rate constant value was 0.01830 g/(mg·min). The adsorption capacity was maximum at pH 6 at room temperature[11].

Activated carbon obtained from banana peels has shown the adsorption of As(III) as 142.86 mg/g. The optimum pH for As(III) adsorption on such activated carbon was at 7 and the experimental data fitted to pseudo second order kinetic model with rate constant value of 0.0111 g/ (mg·min)[12].

The equilibrium adsorption capacity of As^{3+} was found 101.01 mg/g with Fe loaded bentonite and the adsorption process was favored to Langmuir adsorption isotherm model and the adsorption process was controlled by pseudo-

second –order kinetics with the rate constant value 0.03723 g/(mg.min)[13].

The adsorption of Pb(II) ions on natural agricultural waste adsorbents chalf, rice husk, sesame, sunflower and tea waste was carried out. The result showed that the capacities of chalf, rice husk, sesame husk, sunflower husk and tea waste for Pb(II) ion removal were 6.85, 6.38, 6.93, 6.29 and 6.24 mg/g respectively. The results also showed that efficiencies of chalf, rice husk, sesame husk, sun flower husk and tea waste for Pb ion removal were 85, 90, 100, 86 and 98%, respectively. The experimental data were well fitted with Freundlich isotherm model and pseudo first order kinetic model[14].

The Pb ion adsorption study on the activated carbon zeolite composite obtained from coal fly ash was carried out where the optimum pH for Pb(II) ion adsorption was found to be 6 and the equilibrium monolayer adsorption capacity calculated from Langmuir model was 270.27 mg/g[15].

The adsorption of Pb(II) from an aqueous solution on activated carbon obtained from cabbage waste was studied where the maximum adsorption capacity was 54.945 mg/g. The kinetics of the adsorption was described by a pseudo second order model with the rate constant value 0.055 g/(mg·min)[16].

MATERIALS AND METHODS

Preparation of Adsorbent from Spinach Leaves

Spinach leaves were collected from Birgunj, Parsa (Nepal). It was washed thoroughly first with tap water, then distilled water and was left at room temperature for 2-3 weeks for drying. The dried spinach leaves were ground and powder obtained. 15 g dried spinach was kept in the 500 mL of round bottom (RB) flask. 30 mL of *ortho* phosphoric acid was poured in it, while pouring this acid the R.B flask was kept on ice bath. Then condenser was fitted on the RB flask, and heated gently. It was heated at 60- 100 °C for 12, 24 and 36 hours on oil-bath, separately. Thus, three different types of spinach adsorbent materials were obtained. Thus obtained adsorbent was washed with distilled water until it was neutral. This washed sample was kept in oven for drying for 24 hours at 100 °C temperature.

Preparation of stock and standard solutions

Preparation of As(III) solutions

Accurately 1.32 g of arsenic trioxide (As_2O_3, LR Grade, dried at 110 °C for an hour) was dissolved in 5 mL of 10 M sodium hydroxide in a 1000 mL volumetric flask, shaken and the volume was made 1000 mL with distilled water. Working solutions of 1 to 500 ppm were prepared by dilution method.

Preparation of Pb(II) solutions

Accurately 0.8073 g of $Pb(NO_3)_2$ was dissolved 5 mL of concentrated HNO_3 in 1000 mL volumetric flask and diluted with distilled water up to the mark. The obtained stock solution was used for working solutions preparation required for each experiment.

Preparation of methylene blue (MB) solutions

The methylene blue (AR Grade, Qualigens Fine Chemicals, India) was weighed out accurately 1.000 g and transferred to 1000 mL volumetric flask. It was then dissolved with distilled water and diluted up to the mark. The appropriate volume of stock solution was taken to get the working methylene blue solutions of required concentration by dilution method.

Ammonium molybdate reagent (I)

Ammonium heptamolybdate [{$(NH_4)_6Mo_7O_{24}.4H_2O$}, LR Grade] 12.5 g was dissolved in 87.5 mL of distilled water. The 140 mL concentrated sulphuric acid was added to 200 mL of distilled water cautiously. It was cooled and added to the ammonium molybdate solution and diluted to 500 mL.

Ammonium molybdate reagent (II)

Ammonium molybdate (20.05 g) was transferred into 500 mL volumetric flask and dissolved in 250 mL of distilled water. Ammonium molybdate reagent(I) 198 mL was added to the reagent(II), cooled and diluted up to 500 mL with distilled water. The concentration of reagent (II) was 5%.

Working solution of ammonium molybdate

The 10 mL of 5% ammonium molybdate reagent (II) was diluted up to mark in a 100 mL volumetric flask. The final concentration was 0.5 M.

Potassium permanganate solution

Potassium permanganate ($KMnO_4$, LR Grade) 0.790 g was transferred to 250 mL volumetric flask and dissolved in distilled water. The volume was made up to mark. It was stored in dark place. The strength of the solution was 0.1 N.

Sulphuric acid solution (1.5 N)

1.5 N sulphuric acid was prepared by diluting 36.76 N concentrated sulphuric acid to a 250 mL volumetric flask with distilled water.

Hydrazine Hydrate solution

2.44 mL of concentrated hydrazine hydrate was diluted up to mark in 100 mL volumetric flask. The final concentration was 0.5 M.

NaOH (0.1M) and HCl (0.1 M)

Accurately 0.4 g of NaOH was transferred into 100 mL volumetric flask and dissolved with distilled water and diluted up to mark. 0.69 mL concentrated hydrochloric acid was transferred into 250 mL volumetric flask and diluted with distilled water up to mark. The concentration of thus prepared solution was 0.1 M.

Buffer solution

Buffer solutions of pH 4.0, 7.0 and 9.2 were prepared by dissolving buffer tablet of pH 4.0, 7.0 and 9.2 in 100 mL volumetric flasks with distilled water and employed for calibration of pH meter is technical buffer pH 4.0 and 7 of trace model.

Calibration curve for MB solution

For the preparation of calibration curve, at first the maximum absorbance was obtained by finding λ_{max}. Here it was done by preparing 25 mg/L solution of methylene blue. The absorbance was measured against wavelength ranging from 600 to 680 nm using spectrophotometer (2306, Electronics, India). The maximum absorbance was obtained at 665 nm (λ_{max}). After that the methylene blue solutions of 1, 2, 3, 4, 5, 6, 7, 8, 9 and 10 mg/L were prepared in 25 mL volumetric flasks. The absorbance of all these solutions was taken at 665 nm wavelength. A plot of absorbance versus concentration thus gave a calibration curve for methylene blue solution.

Preparation of calibration curves for metal ions

For the preparation of calibration curve of As(III), Arsenic solution containing 1, 2, 3, 4, 5, 6, 8, 9 mg/L and blank solution were prepared in 25 mL volumetric flasks by the method shown in Figure 1.

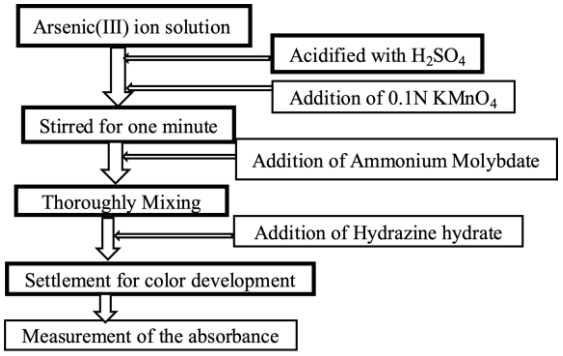

Figure 1: Schematic diagram for quantitative measurement of As(III) ion.

The required amounts of diluted solutions were pipetted out and transferred into 25 mL volumetric flask. To each solution 4.5 mL of sulphuric acid (0.5 N) was added then one drop of potassium permanganate (0.1 N) was added, stirred for one minute. 3 mL of ammonium molybdate (0.5%) and 3 mL of hydrazine hydrate (0.5 M) were added. Then the volume was made up to mark by adding distilled water. The above solutions were left for 20 minutes at room temperature for full colour development. The absorbance of each solution was measured at 840 nm against blank solution with the help of spectrophotometer (2306, Electronics, India). A plot of absorbance versus concentration of arsenic was made.

Lead solution containing 1.0, 5.0 and 10.0 mg/L and blank solution were prepared in 25 mL volumetric flask. The

absorbance of each solution was measured at 282.3 nm against blank solution with the help of AAS (AA-7000, Shimadzu, Japan). A plot of absorbance versus concentration of lead was made.

Specific surface area determination

For determining the specific surface area of spinach adsorbent materials, Langmuir adsorption isotherm model was used. For this, 0.05 g of spinach adsorbent material was transferred to each reagent bottle containing methylene blue solutions of varying concentrations in between 50 to 300 mg/L.

The solutions were then shaken for 24 hours in a mechanical shaker and then allowed to rest for half an hour. After the adsorbent settled down, the supernatant solution was pipetted out. The absorbance of the resultant solution was noted at 665 nm wavelength. From the Langmuir adsorption isotherm, Q_{max} value was calculated. The specific surface area is calculated by following equation[16]:

$$S_{MB} = \frac{N_g \times a_{MB} \times N \times 10^{-20}}{M} \quad \ldots\ldots\ldots \quad (1)$$

Where, S_{MB} is the specific surface area in 10^{-3} km^2 kg^{-1}, N_g is the number of molecules of methylene blue adsorbed at monolayer of adsorbent in kg, a_{MB} is the occupied surface area of one molecule of methylene blue = 197.2 $Å^2$, N is Avogadro's Number (6.023×10^{23}), M is the molecular weight of the methylene blue (319.85 $gmol^{-1}$) and N gives mmol/g which is equivalent to Q_m of the Langmuir equation.

Effect of pH

For the pH of As(III) and Pb(II) adsorption, the initial concentration and volume of solution were taken 20 mg/L and 50 mL respectively. The solutions were taken in 100 mL Erlenmeyer flask and pH of the solutions was adjusted from 2 to 8 using appropriate strength of NaOH and HCl solutions by the help of pH meter. To each flask, 0.05 g spinach adsorbent reflux for 24 hours was added and then shaken in mechanical shaker for 24 hours at speed 220 rpm. After shaking, each solution was filtered immediately using Whatman No. 41 filter paper and the equilibrium pH of the filtrate was noted. The filtrates were analyzed separately to determine the equilibrium concentration of As(III) with the help of UV-Visible spectrometer while for Pb(II) with Atomic Absorption Spectrophotometer.

Adsorption Isotherm Studies

For the study of isotherm studies of As(III) and Pb(II), the effect of arsenic and lead concentrations on the adsorption was studied under optimum pH. The adsorption isotherm studies were done with different initial concentrations of As(III) and Pb(II) ions ranging from 10 to 100 mg/L with 0.05 g of spinach adsorbent reflux for 24 hours. The solutions were shaken in a mechanical shaker for 24 hours at speed of 200 rpm. The equilibrium concentrations of arsenic after adsorption were determined by molybdenum blue method using spectrophotometer while that of lead concentration was determined by Atomic Absorption Spectroscopy (AA-7000, Shimadzu, Japan). Two models Langmuir model and Freundlich model have been tested to study the adsorption isotherm study.

Kinetic Studies

The adsorption kinetics experiments were performed at corresponding optimum pH for As(III) and Pb(II) ions by equilibrating. For this study, 50 mL of 20 mg/L arsenic and lead solutions in 100 mL Erlenmeyer flask containing 0.05 g spinach adsorbent reflux for 24 hours were used separately. These flasks were shaken for different length of time 2 to 120 minutes, in a mechanical shaker at speed of 220 rpm. The kinetics were investigated by taking out flask at desired period of contact time and immediately filtrated through Whatman No. 41 filter paper to obtain filtrates and the concentrations in the filtrates were determined spectrophotometrically. The data obtained was tested with pseudo-first order and pseudo-second order kinetic models.

X-ray Diffraction (XRD) Measurement

The raw spinach and its adsorbent reflux for 24 hours without any adsorption were analyzed for the phase detection using X-ray Diffractometer with monochromatic

CuKα radiation (D2 Phaser Diffractometer, Bruker, Germany) at Nepal Academy of Science and Technology (NAST). The samples were scanned at 2θ from 10 to 80º. The XRD analysis was done to determine the chemical structure of the adsorbent material obtained from spinach.

Fourier Transform Infrared (FTIR) Analysis

All the four samples prepared in different environment, without any adsorption were analyzed by using Fourier Transform Infrared Spectroscopy (IRTracer 100, Shimadzu, Japan) at Central Department of Chemistry, Tribhuvan University for the chemical identification of organic and inorganic material in adsorbent materials prepared from spinach leaves.

RESULTS AND DISCUSSION

Characterization of Adsorbent Materials

X-ray diffraction (XRD) Analysis

The XRD pattern of raw Spinach and the activated carbon obtained after chemical treatment (SA-24) are shown in Figure 2.

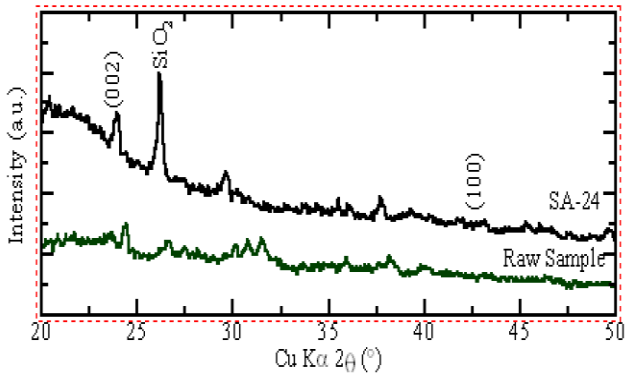

Figure 2: X-ray diffraction patterns of raw and SA-24 samples.

There are two broad diffraction peaks around 2θ = 24° and 43° in XRD pattern of SA-24 sample, corresponding to the diffraction of (0 0 2) and (1 0 0), respectively crystal plane of Carbon.

The sharp diffraction band at 2θ = 26.15° in the SA-24 may be due to the presence of Silica (SiO_2). Thus, from XRD patterns, the present low-cost adsorbent material seemed to contain activated carbon along with silicon dioxide. The presence of silica may be further useful for the removal of another ion in its frame.

Fourier Transform Infra-Red Spectra Analysis

The FTIR spectra of raw spinach and adsorbent prepared from spinach powder refluxed for 12 hours, 24 hours and 36 hours (i.e., SA-12, SA-24 and SA-36) are shown in Figure 3.

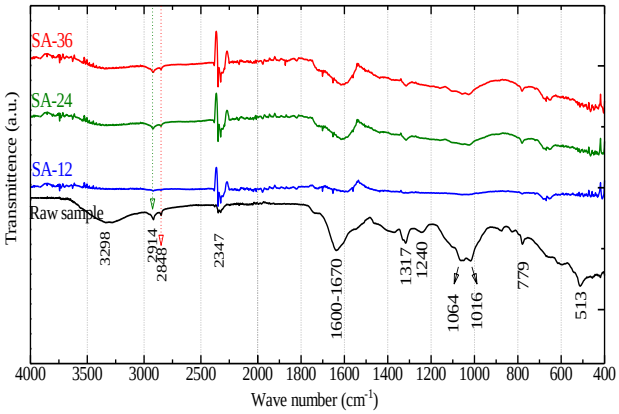

Figure 3: FTIR spectra of raw spinach and adsorbent prepared from spinach powder refluxed for 12, 24 and 36 hours.

The FTIR spectrum of above figure showed that spectrum of spinach adsorbent was not well observed. The spectrum of SA-24 was showed clear bands than SA-12 and SA-36. The FTIR spectrum of activated carbon prepared from spinach showed main absorption at 513, 779, 1016, 1064, 1240, 1317, 1600-1670, 2347, 2848-2914, 3298 cm^{-1} and these peaks were characterized as stretching of C-Br bond of alkyl bromide, bending of =C-H (Carbon-Hydrogen) bond of alkene, stretching of C-O bond of ester, stretching of C-O bond of alcohol or phenol, stretching of C-O bond of ether, bending of –CH bond of alkane, N-H bending of Amine, Adsorbed CO_2, symmetrical and asymmetrical stretching of aliphatic band in C-H (Carbon- Hydrogen) of alkane and Hydrogen-bonded (O-H) of alcohol and phenol, respectively.

The λ_{max} determination and calibration curve of Methylene Blue solution

The maximum absorbance i.e., λ_{max} was obtained at 665 nm with the variation of wavelength and is similar with the previous reports[11, 13]. The linear relationship between the

absorbance and the concentration up to 10 mg/L in the calibration curve of methylene blue solution indicates to follow the Beer Lambert's law.

Specific surface area determination

In order to obtain the specific surface area of the adsorbents prepared from spinach leaves, the linearize Langmuir plots for the adsorption of MB were made and the Langmuir parameters were obtained. Finally, the specific surface area of spinach adsorbents i.e., SA-12 (Reflux for 12 hours), SA-24 (Reflux for 24 hours) and SA-36 (reflux for 36 hours) were calculated using above mentioned equation (1) and were 388, 436 and 388 m^2/g, respectively.

The specific surface area of SA-24 was the highest among these three samples which may be due to the fact that more adsorbents were formed with a greater number of pores in the SA-24 in comparison to SA-12. This also implies that the ash content and other impurities were lower in the SA-24. The lower specific surface area of SA-36 may be due to the overdose of high temperature activation resulting in the formation of more ash content and other impurities that are capable of blocking the pores of the adsorbent[11].

Effect of pH

The effect of pH for the adsorption of As(III) and Pb(II) onto the spinach adsorbent reflux for 24 hours (SA-24) prepared in this study is shown in Figure 4.

The effect of initial pH on the adsorption of As(III) and Pb(II) was studied in the rage from 2 to 8. The adsorptions of As(III) and Pb(II) were found increasing with increasing initial pH value from 2 up to 5 and then decreased with further increase the initial pH.

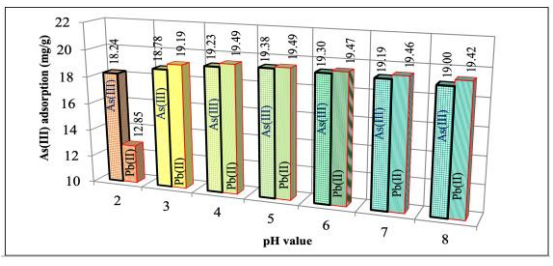

Figure 4: Effect of pH for the adsorption of As(III) and Pb(II) onto the spinach adsorbent SA-24.

The maximum adsorptions of As(III) and Pb(II) were found at initial pH 5 with the values 19.38 and 19.49 mg/g respectively.

The removal of lead by activated carbon from pomegranate peel was studied and found pH 5.6 as optimum pH[17]. And the removal of Lead and Arsenic ions from the aqueous solution has optimum pH at 5 itself[18]. Also other researches have shown the about 5 as optimum pH for the removal of As(III) and Pb(II)[1]. For further experimental works, the adsorption of As(III) and Pb(II) onto the present low-cost adsorbent material, the optimum pH value was set to pH 5.

Batch Adsorption Isotherms of As(III) and Pb(II)

Adsorption isotherm is a graphic representation of the weight of adsorbate adsorbed per unit mass of the adsorbent as a function of the weight of adsorbate left in bulk solution at equilibrium at constant temperature. Langmuir and Freundlich adsorption isotherms are the well-known most popular models used to analyze adsorption behavior.

Langmuir model of adsorption has been applied for the adsorption of solute from a liquid solution on homogeneous adsorbent with the formation of monolayer coverage and adsorption is independent of the occupation of neighboring sites[19]. The Langmuir model is used to determine the maximum adsorption capacity of complete monolayer coverage on the adsorbent surface. The linearized form of Langmuir adsorption isotherm is given as:

$$\frac{C_e}{Q_e} = \frac{1}{Q_m b} + \frac{C_e}{Q_m} \quad \cdots \quad (2)$$

Where Q_e (mg/g) is the weight of adsorbate adsorbed per unit weight of adsorbent at equilibrium, C_e (mg/L) is the equilibrium concentration of the adsorbate, Q_m (mg/g) is the maximum adsorption capacity and 'b' (L/mg) is the Langmuir adsorption equilibrium constant.

A plot of C_e/Q_e against C_e gives a straight line with slope $1/Q_m$ and intercepts $1/Q_m b$ from which Q_m and 'b' can be determined.

Thermodynamic study of adsorption isotherm

Thermodynamic consideration of a adsorption process is necessary to conclude whether the process is spontaneous

or not. The Gibbs free energy change (ΔG^o) is a critical factor for determining the spontaneity of a process. The Langmuir constant b is related to free energy change of adsorption ΔG (kJ/mole) by the relation[20]:

$$\Delta G = -RT\ln(b) \quad \cdots\cdots \quad (3)$$

Where, R = Universal gas constant (8.314 $Jmol^{-1}K^{-1}$), T = Temperature in Kelvin and b is Langmuir constant in (L/mol). Gibbs free energy indicates the degree of spontaneity of adsorption process. More negative value reflects greater energetically favorable process.

The experimental data obtained during adsorption process can also be analyzed with Freundlich adsorption isotherm model which was established in 1939[21]. The linear from of the Freundich isotherm is:

$$\log Q_e = \log K_F + \frac{1}{n}\log C_e \quad \cdots \quad (4)$$

Where Q_e (mg/g) is the amount of adsorbate adsorbed per unit mass of adsorbent, C_e (mg/L) is the equilibrium concentration of the adsorbate, K_F [(mg/g) $(L/mg)^{1/n}$] and n (g/L) are Freundlich equilibrium coefficients, which are considered to be the relative indicators of adsorption capacity and adsorption intensity.

The $\log Q_e$ is plotted against $\log C_e$ a straight line is obtained with slope 1/n and intercept $\log K_F$. From this plot, the value of 1/n and K_F can be determined. The value of 1/n between 0 and 1.0 indicates the favorable adsorption of adsorbate.

Error analysis for isotherm studies

In case of single element isotherm studies, there is the need of error function to optimize the procedure in order to evaluate the fit of the isotherm to the experimental equilibrium data. There are several different error functions[22]. The error functions are the sum of the squares of the errors, the hybrid fractional error function, Marquardt's percent standard deviation, the sum of the absolute errors and chi square test. The best fit among the isotherm models is given by the linear coefficient of determination (R^2) and non-linear Chi square (χ^2)[23]. In this study, the Chi-square test was performed by using the mathematical expression:

$$\chi^2 = \sum \frac{(Q_{e,cal} - Q_{e,exp})^2}{Q_{e,cal}} \quad \cdots\cdots \quad (5)$$

Where $Q_{e,calc}$ is the equilibrium capacity obtained by calculated from model (mg/g) and $Q_{e,exp}$ is the equilibrium capacity (mg/g) from the experimental data. The lower value of χ^2 suggests the best fit model.

Table 1: Parameters of Langmuir and Freundlich constants.

Ions	Langmuir model				
	Q_{max} (mg/g)	b (L/mg)	R^2	ΔG (kJ/mol)	χ^2
As(III)	116.28	0.124	0.9940	-23	2.87
Pb(II)	128.20	0.148	0.9893	-25	0.96
Ions	Freundlich Model				
	K_F [(mg/g)(L/mg)$^{1/n}$]		n	R^2	χ^2
As(III)	13.98		1.50	0.9890	404.5
Pb(II)	17.33		1.51	0.9890	1.49

Adsorption of As(III) and Pb(II) onto Spinach adsorbent reflux for 24 hour (i.e., SA-24) was done by optimizing the pH at 5 and varying the concentrations of Pb(II) and As(III) from 10 to 100 mg/L that gave the linear relationship with Langmuir and Freundlich isotherms. Langmuir and Freundlich parameters obtain from the slope and intercept of the linearized curves of both isotherm models, the coefficient of determinations, values of χ^2 for Langmuir and Freundlich isotherms of As(III) and Pb(II) adsorption and change in free energy during adsorption process are tabulated in Table 1.

Since the R^2 of Langmuir is greater than that of Freundlich, which implies that the experimental data fitted well with the Langmuir model. The Q_{max} values obtained from Langmuir model for As(III) and Pb(II) were 116.28, 128.20 mg/g respectively, which are significantly higher than those obtained for the bioadsorbents and mineral adsorbents and the values of χ^2 for the Langmuir model was smaller than

that of the Freundlich model which concludes that adsorption of As(III) and Pb(II) on activated carbon followed the Langmuir adsorption isotherm. And the adsorption of As(III) and Pb(II) ions onto spinach adsorbent is monolayer and involved the adsorption on homogeneous active surfaces.

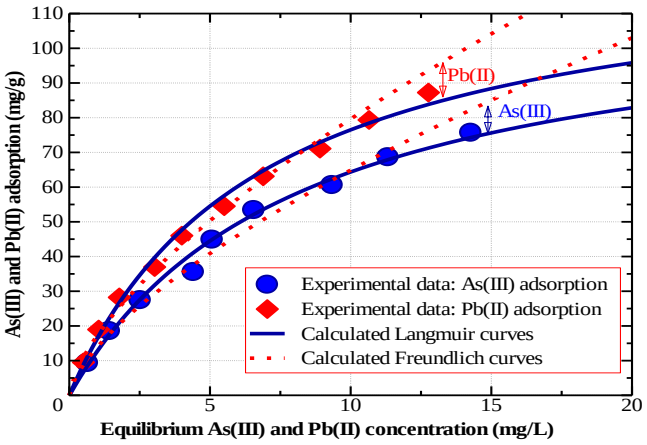

Figure 5: The adsorption isotherms of As(III) and Pb(II) onto adsorbent SA-24.

The values of ΔG were calculated which were -23 and -25 kJ/mol for As(III) and Pb(II) adsorption respectively. The negative values of free energy (ΔG) in adsorption process reveals the spontaneous nature and feasibility of the adsorption process for the adsorption of As(III) and Pb (II) onto spinach adsorbent. The values of ΔG further confirms the adsorption process is favored by physio-chemical-adsorption for As(III) and Pb(II). From the Langmuir and Freundlich parameters, the adsorption of As(III) and Pb(II) as a function of equilibrium concentrations of As(III) and Pb(II) is shown in Figure 5. The curves are shown that experimental data followed very well with Langmuir model.

Batch Kinetic Studies

The kinetic study reveals the rate and mechanisms of reaction coupled with determination of rate and mechanism of reaction coupled with the determination of rate controlling step. In the study pseudo-first-order and pseudo-second-order models have been studied to find out the limiting step of As(III) and Pb(II) ions adsorption.

The differential form of pseudo-fist order rate equation, applicable for the reversible reaction, is generally expressed as[24]:

$$\frac{dQ_t}{dt} = K_1(Q_e - Q_t) \quad \cdots \quad (6)$$

Where, Q_e (mg/g) is the amount of adsorbate adsorbed at equilibrium and Q_t (mg/g) is the amount of adsorbate adsorbed at time 't'. The term K_1 (min^{-1}) is the rate constant of pseudo-first order adsorption.

After integration and applying boundary condition, t = 0 to t and Q_t = 0 to Q_t the linearized from of equation becomes:

$$\log(Q_e - Q_t) = \log Q_e - \frac{K_1}{2.303}t \quad \cdots \quad (7)$$

The plot of log (Q_e - Q_t) versus 't' will give a straight line from which K_1 and Q_e can be determined from slopes and intercepts of the plot respectively.

The pseudo-second order kinetic model is used to study the kinetics of adsorption of adsorbate and it states that the rate of occupation of adsorption sites is proportional to the square of the number if unoccupied sites[25]. It is generally expressed as:

$$\frac{dQ_t}{dt} = K_2(Q_e - Q_t)^2 \quad \cdots \quad (8)$$

Where K_2 (g/mg·min) is the pseudo-second order rate constant and Q_e and Q_t are the amount of adsorbate adsorbed at equilibrium and any time 't' respectively.

With integration and applying boundary conditions, t=0 to t and Q_t = 0 to Q_t the equation becomes:

$$\frac{1}{Q_t} = \frac{1}{K_2 Q_e^2} + \frac{1}{Q_e}t \quad \cdots\cdots\cdots \quad (9)$$

If the initial adsorption rate is V_0 (mg/g min), then

$$V_0 = K_2 Q_e^2 \quad \cdots \quad (10)$$

The equation can also be written as:

$$\frac{1}{Q_t} = \frac{1}{V_0} + \frac{1}{Q_e}t \quad \cdots \quad (11)$$

The values of Q_e and K_2 can be determined from the linear plot of t/Q_t versus 't' with the slope and intercept of the plot respectively.

The effect of contact time and two models (pseudo-first order and pseudo-second order) were employed to the experimental kinetics data as shown in Figures 6 and 7.

The rate of reactions as well as the maximum adsorption capacities obtained from the slopes and intercepts of the Figures 6 and 7 are tabulated in Table 2.

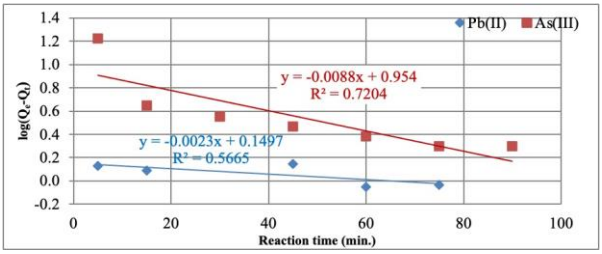

Figure 6: Pseudo-first order kinetic model for the adsorption of As(III) and Pb(II) ion onto adsorbent SA-24.

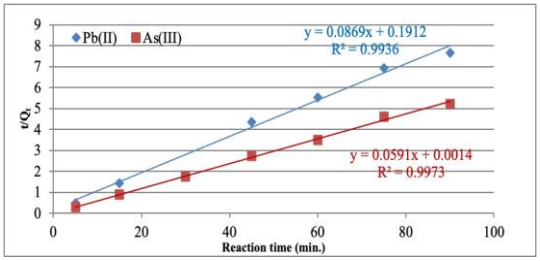

Figure 7: Pseudo-second order kinetic model for the adsorption of As(III) and Pb(II) ion onto adsorbent SA-24.

Table 2: Kinetic parameters for adsorption of As(III) and Pb(II) onto adsorbent SA-24.

	1st order		2nd order	
Ion	As(III)	Pb(II)	As(III)	Pb(II)
Slope	0.0088	0.0036	0.0591	0.0869
Intercept	0.9540	0.1497	0.0014	0.1912
K_1	0.020	0.008		
K_2			2.495	0.039
Q_t	02.596	01.161	16.920	11.507
R^2	0.7204	0.5665	0.9973	0.9936

The coefficient of determination values of pseudo- first order and pseudo-second order models of As(III) and Pb(II) were 0.7204, 0.5665 and 0.9973, 0.9936, respectively showed that the kinetics of As(III) and Pb(II) ion onto adsorbent SA-24 followed pseudo-second order kinetics. The kinetic plots of the adsorption of As(III) and Pb(II) are shown in Figure 8 where the solid line curves are calculated curves using maximum adsorption capacity and the rate of reaction of pseudo-second order kinetics obtained from Table 2.

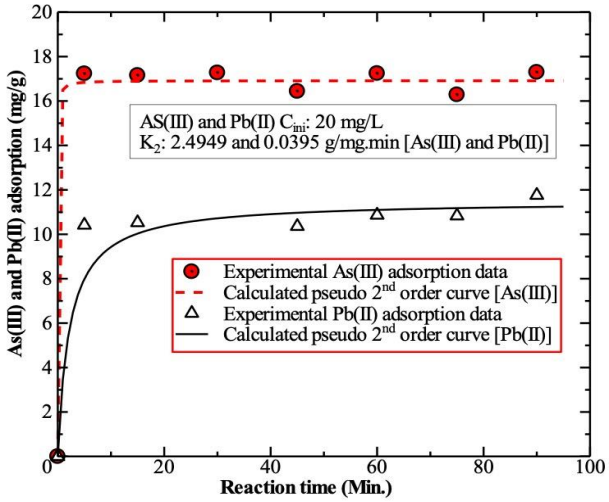

Figure 8: Kinetic plots for the adsorption of As(III) and Pb(II) on adsorbent SA-24.

It is clear from the Figure 8 that initially up to 5-10 minutes reaction time the process of adsorption was rapid and the equilibrium reached within 30 minutes and nearly 45 minutes for As(III) and Pb(II) respectively. After reaching the saturation point there was no significant change in the rate of adsorption. The initial rapid increase in the rate was due to the availability of more number of active sites so that large number of As(III) and Pb(II) ion got attached to adsorbent sites. As the time passed, the number of active sites became less and finally the equilibrium state was reached.

Mechanisms of As(III) and Pb(II) Adsorption

Intraparticle diffusion model is applied to gain insight into the mechanisms and rate controlling steps affecting the

kinetics of adsorption. The kinetic results are fitted to Weber-Morris equation[26]:

$$Qt = K_{id}t^{0.5} + C \quad \cdots\cdots (12)$$

Where C is the intercept and K_{id} (mg/g $h^{0.5}$) is the intraparticle diffusion rate constant, which can be evaluated from the slope of the linear plot of Q_t versus $t^{0.5}$. The intercept of the plot reflects the boundary layer effect. The larger the intercept, the greater is the contribution of the surface sorption in the rate-controlling step. If the regression of Q_t versus $t^{0.5}$ is linear and passes through the origin, then intraparticle diffusion is the sole rate-limiting step. When the plots do not pass through the origin, this indicates some degree of boundary layer control and these further shows that the intraparticle diffusion is not the only rate-determining step but other kinetics models may also control the rate of adsorption.

The graphical relationship between the amount of As(III) and Pb(II) adsorbed (mg/g) as a function of square root of time (√t) is shown in Figure 9.

The plot of Q_t verses √t does not pass through the origin and indicates that the intra-particle diffusion model was not the rate limiting step.

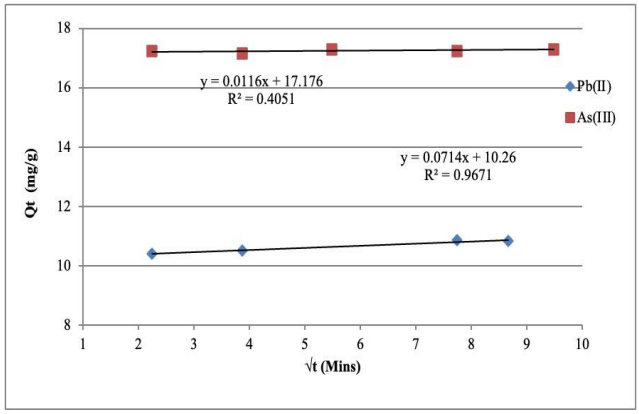

Figure 9: Plot of Q_t verses √t for the adsorption of As(III) and Pb(II) on adsorbent SA-24.

Furthermore, the FTIR analysis of SA-24 after the adsorption of As(II) and Pb(II) was carried and is shown in Figure 10.

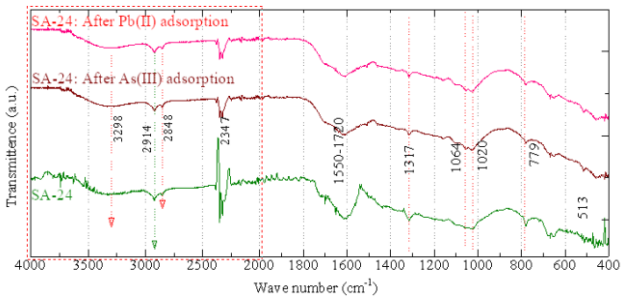

Figure 10: FTIR spectra of the adsorbent SA-24, after adsorptions of As(III) and Pb(II) ions.

No any broad band of hydroxyl peaks was detected in the spectra obtain after the adsorption of As(III) and Pb(II) ions in the range of 3500-3000 cm^{-1}. This diminished of hydroxyl peak after adsorption may be due to involvement of hydroxyl group in the adsorption process. Peaks of CO_2 seen at 2347 was mostly diminished after both ions adsorption showing that both ions were perfectly adsorbed on the adsorbent expelling out CO_2 from their adsorbent sites.

Comparison of Maximum Adsorption Capacities

Comparison of the maximum adsorption capacity (Q_{max}) of the Spinach adsorbent reflux for 24 hours (i.e., SA-24) for As(III) and Pb(II) with earlier investigated adsorbents are tabulated in Table 3.

Table 3: Comparison of maximum adsorption capacity (Q_{max}) with earlier investigated adsorption.

S. N.	Adsorbent	Q_{max} (mg/g)		Source
		As(III)	Pb(II)	
1.	Phosphorylated Orange juice residue	68.18		27
2.	Zr(IV) loaded saponified orange waste gel	130		28
3.	Fe loaded pomegranate waste	50		29
4.	Iron-impregnated granular activated carbon	1.95		30
5.	Spinach adsorbent (H_2SO_4 activated)	58.480		11

S. N.	Adsorbent	Q_{max} (mg/g)		Source
		As(III)	Pb(II)	
6.	Steam activated banana peels	142.86		12
7.	Fe-bentonite	101.01		13
8.	Chicken Bone	96.153	163.91	18
9.	Activated carbon zeolite composite		270.27	15
10.	Activated carbon (cabbage waste)		54.945	1
11.	Sunflower husk		6.29	14
12.	Tea waste		65	31
13.	Egg shell		154	6
14.	Spinach adsorbent	116.279	128.205	Present work

The results revealed that Spinach adsorbent possesses higher potentiality towards the adsorptive removal of As(III) than Pb(II) from synthetic wastewater solution.

Conclusions

The specific surface areas of three different adsorbents namely SA-12, SA-24 and SA-36 were 388, 436 and 388 m^2/g, respectively. The maximum adsorption capacities of As(III) and Pb(II) were 116.28 mg/g and 128.20 mg/g at optimum pH 5 onto adsorbent SA-24 and the adsorption fitted well with the Langmuir isotherm.

The rate of adsorption was fast up to 10 min and then it was slowed down. The equilibrium contact time was 30 min for arsenic and nearly 45 min for lead. The kinetics of the adsorption onto SA-24 was found to follow pseudo second order model with rate constant value 2.495 and 0.039 g/(mg. min) for As and Pb ions, respectively. The test for intraparticle diffusion model showed that the adsorption of As(III) and Pb(II) onto SA-24 was not solely intraparticle diffusion.

The above experimental data of the effect of pH, change in free energy during the process of adsorption indicate that process of adsorption of As(III) and Pb(II) onto the present low cost adsorbent material is complex and may involve more than one mechanism. The adsorption process is physiorption along with chemisorption with the ion exchange with the available exchangeable cations present in the adsorbent material.

Acknowledgements

First author (B.K. Das) is thankful to University Grants Commission (UGC) for providing Master's Thesis Support for this research work (The UGC Master Research Support Award No.: MRS/74_75/S&T-22). We are grateful to Dr. Suresh Kumar Dhungel of Nepal Academy of Science and Technology (NAST) for the support to get X-ray diffraction measurement of my samples. We are thankful to Mr. Ram Bahadur Gharti from Department of Mines and Geology for providing Atomic Absorption Spectrophotometer (AAS) for elemental analysis of lead.

References

1. Paneru, K. R. and Jha, V. K. 2020. Adsorptive removal of Pb(II) ions from aqueous solution by activated carbon prepared from cabbage waste. *Nepal Journal of Environmental Science*. **8**(1):1-10. Doi: https://doi.org/10.3126/njes.v8i1.34446
2. Global Health and education foundation. 2007. https://www.koshland-science-museum.org/water/new/en/Overview/Why-is-Safe-Water-Essential.html) (Accessed on 11 May, 2019).
3. Pandey, S. 2006. Water pollution and health. *Kathmandu University Medical Journal*. **4**(1): 128-134.
4. Pantha, K et al. 2021. Faecal pollution source tracking in the holy Bagmati River by portable 16S rRNA gene sequencing. *npj Clean Water*. **4**: Article No. 12. Doi: https://doi.org/10.1038/s41545-021-00099-1
5. Hirota, M., Higaki, S., Higaki, T. and Hasezawa, S. 2013. Investigation of contamination in spinach collected immediately following the Fukushima Daiichi nuclear disaster. *Radiation Safety Management*. **12**(2): 43-47.
6. Gandhi, N., Sirisha, D., Shekar, K. C. and Asthana, S. 2012. Removal of fluoride from water and waste water by using low-cost adsorbents. *International Journal of ChemTech Research*. **4**(4): 1646-1653.
7. Codling, E. E. 2014. Accumulation of lead and arsenic by lettuce grown on lead-arsenate contaminated orchard soils. *Open Agriculture Journal*. **8**: 35-40.
8. Hanaa, S. M., Abd. El-Rahman., Abeer M. N., H. El-Dakak. and Zein H. 2015. Investigation and evaluation on heavy metal contaminations of green salads and potato fried in different restaurants and fresh vegetables in some Egyptian governorates.

International Journal of Environmental Monitoring and Analysis. **3**(2): 28-37.

9. Znad, H. and Frangeskides, Z. 2014. Chicken drumstick bones as an efficient biosorbent for copper (II) removal from aqueous solution. *Desalination and Water Treatment*. **52**(7-9): 1560-1570.
10. Roy, P. et al. 2013. Removal of arsenic (III) and arsenic (V) on chemically modified low-cost adsorbent: batch and column operations. *Applied Water Science*. **3**(1): 293-309.
11. Jha, P. K and Jha, V. K. 2021. Arsenic adsorption characteristics of adsorbent prepared from Spinacia oleracea (Spinach) leaves. *Scientific World*. **14(**14): 51–61.
    Doi: https://doi.org/10.3126/sw.v14i14.34987
12. Maharjan, J. and Jha, V. K. 2022. Activated carbon obtained from banana peels for the removal of As (III) from water. *Scientific World*. **15**(15): 145–157.
    Doi: https://doi.org/10.3126/sw.v15i15.45665
13. Yadav, B. K. and Jha, V. K. 2023. Incorporation of Fe(III) into bentonite and study of its As^{3+} adsorption properties. *Scientific World*. **16**(16): 38–49.
    Doi: https://doi.org/10.3126/sw.v16i16.56767
14. Surchi, K. M. S. 2011. Agricultural wastes as low cost adsorbents for Pb removal: kinetics, equilibrium and thermodynamics. *International Journal of Chemistry*. **3**(3): 103-112.
    Doi: 10.5539/ijc.v3n3p103.
15. Regmi, M. and Jha, V. K. 2019. Synthesis and Characterization of Activated Carbon Zeolite Composite from Coal Fly Ash for Pb (II) removal from Aqueous Solution. *Journal of Environment Science*. **V**: 170-178.
16. Itodo A. U., Itodo, H. U. and M. K. Gafar. 2010. Estimation of specific surface area using Langmuir isotherm method. *Journal of Applied Sciences and Environmental Management*. **14**(4): 141-145.
17. El-Ashtoukhy, E. S., Amin, N. K. and Abdelwahab, O. 2008. Removal of lead (II) and copper (II) from aqueous solution using pomegranate peel as a new adsorbent. *Desalination*. **223**(1-3): 162-173.
18. Upreti R. 2018. To prepare law cost adsorbent materials from chicken bone and study the removal of toxic ions (lead and arsenic) from synthetic wastewater. *M.Sc. Dissertation. Central Department of Chemistry, Tribhuvan University*.
19. Langmuir, I. J. 1918. The adsorption of gases on plane surfaces of glass, mica and platinum. *Journal of the American Chemical Society*. **40**: 1361-1403.
20. Aryal, M., Ziagova, M. and Liakopoulou, K. M. 2011. Comparasion of Cr (VI) and As (V) removal is single and binary mixtures with Fe (III) treated Staphylococcus xylosus Biomass: Thermodynamic studies. *Journal of Chemical Engineering.* **169**: 100-106.
21. Freundlich, H. and Heller, W. 1939. The Adsorption of cis- and trans-Azobenzene. *Journal of American Chemical Society*. **61**: 2228-2230.
22. Ng, J., Cheung, W. and McKay, G. 2002. Equilibrium studies of the sorption of Cu (II) ions onto chitosan. *Journal of Colloid and Interface Science.* **255**(1): 64-74.
23. Agarwal, A. K., Kadu, M. S., Pandhurnekar, C. P. and Muthreja, I. L. 2014. Langmuir, Freundlich and BET Adsorption Isotherm Studies for Zinc ions onto Coal Fly ash. *International Journal of Application or Innovation in Engineering and Management.* **3**(1): 64-71.
24. Lagergren, S. 1898. Zur theorie der sogenannten adsorption geloster stoffe. Kungliga svenska vetenskapsakademiens. *Handlingar*. **24**: 1-39.
25. Ho, Y. S. and McKay, G. 1999. Pseudo-second order model for sorption processes. *Process Biochemistry*. **34**(5): 451-465.
26. Weber, W. J. and Morris, J. C. 1963. Kinetics of adsorption on carbon from solution. *Journal of Sanitary Engineering Division.* **89**(2): 31-60.
27. Ghimire, K. N. et al. 2003. Adsorptive separation of arsenate and arsenite anions from aqueous medium by using orange waste. *Water Research*. **37**(20): 4945-4953.
28. Biswas, B. K. et al. 2008. Adsorptive removal of As(V) and As(III) from water by a Zr(IV)-loaded orange waste gel. *Journal of Hazardous Materials*. **154**: 1066-1074.
29. Thapa, S. and Pokhrel, M. R. 2012. Removal of As(III) from aqueous solution using Fe(III) loaded pomegranate waste. *Journal of Nepal Chemical Society*. **30**: 29-36.
30. Chang, Q., Lin, W. and Ying, W. C. 2010. Preparation of iron-impregnated granular activated carbon for arsenic removal from drinking water. *Journal of Hazardous Materials.* **184**(1-3): 515-522.
31. Amarasinghe, B. M. W. P. K. and Williams, R. A. 2007. Tea waste as a low cost adsorbent for the removal of Cu and Pb from waste water. *Chemical Engineering Journal.* **132**: 299-307.